JURNAL PENATAAN RUANG
Volume 21 Nomor 1, Mei, 2026
P-ISSN 1907-4972 | E-ISSN 2716-179X
DOI: https://doi.org/10.12962/j2716179X.v21i1.4424

Spatial Interaction Analysis Based on Urban Growth Simulation in South Gresik District

R A W D Syafitri✉ [1], A Jatayu[1], P T Setyasa[2], A W Pramesti[1], A Marsa[1],

[1]Department of Urban and Regional Planning, Sepuluh Nopember Institute of Technology, Surabaya, Indonesia

[2]School of Built Environment, University of New South Wales Sydney, Sydney, Australia

Received: 25/05/2025 | Reviewed: 03/02/2026 | Accepted: 15/06/2026

✉rivan@its.ac.id

Abstract: Southern Gresik is undergoing rapid peri-urban transformation as residential and industrial development extends from the Greater Surabaya metropolitan core. This study examines how projected land-cover change may reshape population distribution and spatial interaction across the road network. A cellular automata model was used to simulate land cover from 2022 to 2042 using accessibility variables, neighbourhood effects, AHP-derived weights, and spatial constraints. The projected land-cover map was then combined with dasymetric population redistribution and a network-based gravity model. The simulation achieved an overall accuracy of 83%. By 2042, industrial land is projected to increase from 2.54 to 4.79 ha (+88.6%) and settlement from 9.00 to 12.44 ha (+38.2%), while agriculture declines from 10.72 to 6.71 ha (−37.4%) and vegetation from 5.58 to 3.90 ha (−30.1%). Driyorejo remains the largest population centre, but faster growth is projected in Kedamean (1.58%/year) and Menganti (1.39%/year). Spatial interaction increases more rapidly than population, with regional annual growth rates of 1.95% and 1.01%, respectively, and becomes concentrated along Jalan Raya Kedamean, Driyorejo, and Petiken. The findings indicate that peri-urban growth in Southern Gresik is producing a coupled shift in land use, population location, and corridor dependence, requiring coordinated land-development control and transport planning.

Keywords: cellular automata; gravity model; peri-urban growth; population distribution; spatial interaction

1. Introduction

Urban growth in rapidly urbanising countries has become faster, more dispersed, and more spatially complex than the planning systems designed to anticipate it (Güneralp et al., 2020; Seto et al., 2012). This shift is particularly visible in Asia, where the post-1990s reorganisation of urban growth toward the metropolitan fringe has produced extended desakota landscapes — hybrid regions in which agricultural and urban land uses interweave along corridors linking the city core to its hinterland (Hudalah & Firman, 2012; Mcgee, 1991; Winarso et al., 2015). Indonesian metropolitan regions illustrate this pattern with particular intensity. The peri-urban districts surrounding Jakarta, Bandung, and Surabaya have absorbed disproportionate shares of new settlement and industrial activity over the past two decades(Firman, 2009, 2017; Rustiadi et al., 2021). Anticipating where this growth will occur next, and what it implies for movement between zones, is therefore a central concern for regional planning rather than a peripheral one.

Urban growth in such peri-urban contexts is not simply an additive process of built-up gain; it simultaneously redistributes population and reconfigures the geography of opportunity that determines how zones interact (Geurs & van Wee, 2004; Tobler, 1970). Land cover–transport interaction (LUTI) theory captures this coupling. The configuration of households, jobs, and infrastructure defines what is reachable from where, and that geography of opportunity in turn shapes movement between zones (Acheampong & Silva, 2015; Geurs & van Wee, 2004; Iacono et al., 2008; Wegener, 2004). When urban growth alters these terms — by introducing new residential clusters or industrial estates — inter-zonal interaction shifts in response (Fotheringham & O'Kelly, 1989; Haynes & Fotheringham, 1984; Wilson, 1971). Translating that shift into a calibrated transport-demand forecast, however, requires behavioural inputs such as trip rates, mode shares, and network assignment that are rarely available alongside urban growth simulation outputs in developing-country settings (Barbosa et al., 2018; Lenormand et al., 2016). Where such data are absent, a more defensible analytical strategy is to estimate spatial interaction potential through a gravity formulation, in which interaction is read as a relative function of origin mass, destination mass, and impedance rather than as observed flow (Haynes & Fotheringham, 1984; Roy & Thill, 2004; Wilson, 1971). Alternative population-driven formulations such as the radiation model exist (Simini et al., 2012), but the gravity framework remains the most widely used in planning-oriented contexts where calibration data are limited. The output is a planning indicator of how strongly zones are likely to be coupled, not a forecast but a distinction with direct interpretive consequences.

Urban growth simulation provides the spatial substrate on which such an interaction analysis can be constructed. Since the foundational linking of cellular geography to urban dynamics (Couclelis, 1985; Tobler, 1970), cellular-automata (CA) models have become the dominant family of tools for predicting how cities grow, by translating land suitability, neighbourhood effects, and projected demand into spatially explicit conversion scenarios (Batty & Xie, 1994; Clarke et al., 1997; White & Engelen, 1993). Subsequent generations of the framework incorporated constrained allocation, machine-learning-derived transition rules, and stochastic calibration to improve realism in heterogeneous landscapes (X. Li & Yeh, 2000, 2002; Verburg, Schot, et al., 2004; Wu, 2002). The most recent advances place stronger emphasis on patch-based growth and demand-driven allocation, so that scenarios can be interpreted as planning instruments rather than black-box outputs (Liang et al., 2021; Lin et al., 2023; Liu et al., 2017; Santé et al., 2010). The land cover change modelling platform used in this study follows the same planning-oriented logic, allowing the analyst to specify driving factors, constraints, and projected growth targets (Pratomoatmojo, 2018a). Whatever the platform, however, the credibility of any urban prediction rests on accuracy assessment. Without validation against observed change, scenarios risk being read as deterministic outcomes when they should remain conditional projections (Pontius & Millones, 2011; Van Vliet et al., 2011; Verburg, Schot, et al., 2004).

Southern Gresik occupies the southern arc of the Greater Surabaya metropolitan system and is designated by regional spatial planning policy as a corridor for integrated settlement and industrial development (Gresik Regency Government, 2011; JICA, 2007). Its proximity to the Surabaya core and its position on the regional toll-road network create exactly the conditions under which residential and industrial growth can reorganise the interaction field between local centres and the metropolitan core (Firman, 2009; Hudalah & Firman, 2012; Rustiadi et al., 2021). Yet the published evidence on Indonesian peri-urban areas largely stops at projecting future built-up extent. Studies that proceed further tend either to discuss the consequences for inter-zonal interaction qualitatively or to overreach into uncalibrated trip-demand claims that the available data cannot support (Acheampong & Silva, 2015; Verburg, Schot, et al., 2004). The evidence base for *scenario-based interaction analysis*, framed explicitly as potential rather than as forecast, therefore remains thin in the Indonesian peri-urban literature. This study addresses that gap. It (i) simulates land-cover change in Southern Gresik between 2022 and a 2042 horizon using a calibrated and validated CA framework, (ii) translates the projected population redistribution into a gravity-based estimate of inter-zonal interaction potential, and (iii) interprets the projected changes as a planning signal rather than as a transport-demand forecast. The novelty of this study lies in the integration of these three steps within a single, methodologically consistent workflow for peri-urban metropolitan planning, a configuration that, to the authors' knowledge, has not previously been applied to the southern Surabaya–Gresik corridor.

2. Methodology

2.1. Research Framework

The methodology addresses three analytical objectives: simulating urban land-cover change between 2022 and 2042, validating the simulation against observed historical change, and comparing gravity-based spatial interaction potential between the 2022 baseline and the 2042 scenario (Figure 1). The workflow follows three sequential stages — data preparation, CA-based urban growth simulation with validation, and gravity-based interaction analysis — applied in parallel to the existing condition and the future scenario. Validation acts as a gate: the 2042 land cover is admitted into the interaction analysis only after the CA model reproduces observed land-cover change to an acceptable accuracy. Both the 2022 and 2042 gravity models receive population distributions derived from their respective land covers, ensuring that interaction is estimated from population mass rather than directly from land-cover maps. Gravity-model outputs are interpreted as relative measures of spatial interaction potential under each scenario, not as calibrated travel-demand forecasts.

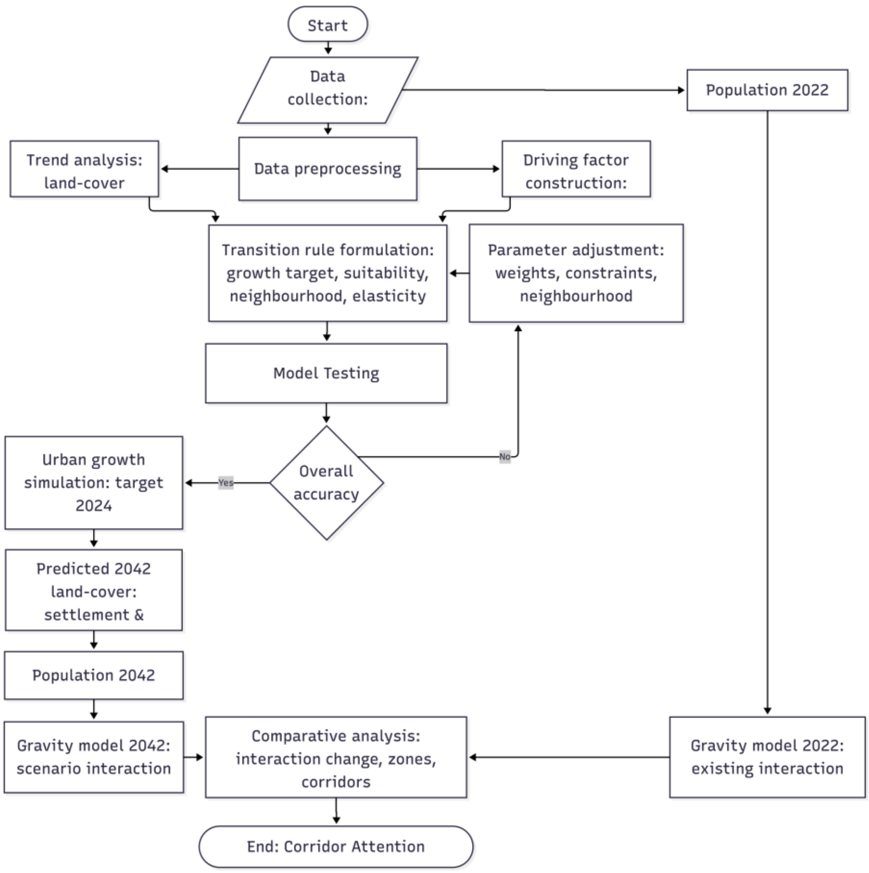

Figure 1. Research workflow

2.2. Data Collection and Preparation

The study combines spatial inputs and zoning with non-spatial inputs. Explicit drivers reflect the principle that land-cover change is shaped by accessibility, agglomeration, and neighbourhood effects under regulatory constraint (Aburas et al., 2016; Liu et al., 2017; Santé et al., 2010). All layers share a common coordinate system and uniform cell size. Drivers are normalised into suitability values, constraints encoded as restriction layers, and the zoning system held constant across both years.

Table 1. Data requirements and analytical functions

No	Data Variable	Variables	Analytical Function	Source
1	Baseline Land Cover	Settlement, Industry, water body, vegetation, agriculture, open public space	Initial state for urban growth simulation and reference map for validation	Landsat Imagery 2002 and 2022
2	Population	Population by pixel, historical growth, projected population	Estimating settlement land requirement and interaction mass	Central Statics Agency Document 2002-2022; World Population 2022
3	Accessibility drivers	Distance to roads, toll gates, activity centres, public facilities, industrial areas	Suitability surface for land conversion	Gresik Regency Spatial Planning Document, 2022 - 2042
4	Constraints	Protected areas, water bodies, disaster-prone zones, restricted land	Limiting or preventing land conversion	Gresik Regency Spatial Planning Document, 2022 – 2042; Inarisk.com; Gresik National Land Agency
5	Spatial interaction zones	Origin and destination zones, centroid, distance or travel impedance	Gravity-model input and comparison unit	Population existing data 2022 and prediction 2024

2.3. Land Cover Change Simulation

The first objective is to simulate land cover change in South Gresik District by allocating future growth cells to locations with the highest transition potential. Technically, the model follows a raster-based cellular automata structure in which each cell has a discrete land cover state, a set of spatial attributes, and a transition probability influenced by local and regional conditions. This structure is consistent with urban CA literature, where spatial change is produced by the interaction between suitability, neighbourhood configuration, constraints, and demand allocation (Clarke et al., 1997; Liu et al., 2017; White & Engelen, 1993). The initial land-cover, growth estimation, driving factors and constraints combined in the set of transition rules to get transition potential map (TP) as direction of simulated urban growth (Pratomoatmojo, 2018a).

$$TP_{i_{x,y}} = \sum_{z=0}^{n}(N_{i_{(z\to n)x,y}} . ITP_{i_{(z\to n)_{x,y}}}) \quad (1)$$

$TP_{i_{x,y}}$ = Transition potential value of land cover i on certain cell (x,y) (sum operation filter)

$N_{i_{(z\to n)x,y}}$ = Neighborhood filter process by certain filter and its accumulation in to center of the cell (x,y), while n is total number of neighborhood cell with or without cell center.

$ITP_{i_{(z\to n)}}$ = Initial transition potential map value for certain land use i. or it can be represented by suitability map for certain land use to grow.

The initial transition potential map or suitability component is calculated from weighted driving factors:

$$ITP = \sum_{m=1}^{n} w_{m,k} X_{i,m}, \qquad \sum_{m=1}^{n} w_{m,k} = 1, \quad (2)$$

where $X_{i,m}$ is the normalised value of driving factor *m* at cell *i*, and $W_{m,k}$ is the weight of factor *m* for land cover transition *k*. Driving factors may include proximity to arterial roads, toll gates, industrial areas, public facilities, existing settlements, and planned development centres.

The suitability component is calculated from weighted driving factors, and the weights are derived using the Analytic Hierarchy Process (AHP) because AHP is commonly used to translate expert judgement on multiple planning criteria into a structured set of relative priorities (Z. Li et al., 2018; Saaty & Vargas, 2012). In this report, AHP is used to weight land-conversion suitability factors. Experts compare pairs of driving factors using Saaty's 1-9 importance scale. These comparisons in our research were obtained by consulting with a team of 3 experts, including academics, governments and transportation planning expert. The consistency check of the pairwise comparison matrix was checked. The consistency check formula is:

$$IC = \frac{\lambda_{max}^{(k)} - n}{n-1} \quad , RC = \frac{IC}{IR} \tag{3}$$

IC measures the internal inconsistency of the pairwise comparison matrix, IR represents the average inconsistency expected from a random matrix of the same size, and RC expresses whether the expert judgement is consistent enough to be accepted (Saaty & Vargas, 2012). The comparison matrix is accepted when $RC<0.1$; otherwise, the pairwise judgements are revised until the consistency threshold is satisfied (Z. Li et al., 2018).

The target growth requirement is estimated using population-based land demand. For settlement land, the required number of additional cells can be written as:

$$G = \frac{A_k^{req} - A_k^{base}}{a_{cell}}, \tag{4}$$

where G is the number of required growth cells for land cover type k, A_k^{req} is the required future land area, A_k^{base} is the baseline land area, and α_{cell} is the area represented by one raster cell. The required build up areas is derived from projected population, it can be estimated as:

$$A_{build-up}^{req} = \frac{P_{2042}}{D_{build-up}}, \tag{5}$$

where P_{2024} is projected population and $D_{build-up}$ is the assumed settlement population density. The model allocates growth cells with the highest transition potential until the target G is fulfilled

To process of Cellular Automata iteration to simulate the urban growth generated by mathematical expression bellow (Pratomoatmojo, 2018b, 2018a). In here will be calculate using LanduseSim software:

$$LU_{i_{x,y}}^{t+1} = f(LU_{x,y}^{t}, TP_{i_{x,y}}, G_{i_{x,y}}, C_{i_{x,y}}, E_{i_{x,y}}, Z_{i_{x,y}}, TS) \tag{6}$$

$LU_{i_{x,y}}^{t+1}$	=	The new growth (change state) of land cover i at the time t+1 on certain cell (x,y)
$LU_{x,y}^{t}$	=	the state of the previous land use class before simulated on certain cell (x,y).
$TP_{i_{x,y}}$	=	Transition potential map of land cover i on certain cell (x,y).
$G_{i_{x,y}}$	=	Number of expected cell growth from land cover/land-cover i at the time t+1.
$C_{i_{x,y}}$	=	Elasticity of change for certain land use to be converted to land use (i).
$E_{i_{x,y}}$	=	Land growth constraint that can be represented of certain land use that can't be converted by land use i or zoning that need to be conserved or protected. Constraint area usually is used to represent such as certain land use class that not possible to be converted by land use i.
$Z_{i_{x,y}}$	=	Zoning system such as land use plan, disaster area, growth promotion zone.
TS	=	Time-step of cellular automata iteration. In here is used 1 iteration

2.4. Land cover Model validation

Validation is necessary because a future scenario is only defensible if the model can first reproduce an observed spatial pattern under known conditions. The validation procedure follows standard land-cover accuracy assessment, where the simulated map and observed reference map are cross-tabulated cell by cell (Congalton, 1991; Foody, 2002). In this study, validation can be implemented through backcasting: the model is calibrated using an earlier baseline map, then used to simulate a known year, and the simulated map is compared with the observed map. This approach also responds to recent criticism that land-change models should report transparent agreement and disagreement measures rather than presenting future maps without empirical evaluation (Pontius & Millones, 2011; Van Vliet et al., 2011). The overall accuracy is calculated as:

$$OA = \frac{\sum_{k=1}^{r} n_{kk}}{N} \times 100\,\%\,, \tag{7}$$

where *OA* is overall accuracy, n_{kk} is the number of correctly classified cells for class *k* on the diagonal of the confusion matrix, *r* is the number of land cover classes, and *N* is the total number of validation cells.

2.5. Population Distribution Model

Population distribution can be refined from coarse-resolution products from WorldPop using a multi-class weighted dasymetric mapping approach, in which land cover classes act as ancillary variables for reallocating population into finer pixels. Following Liu et al. (2023), the population distribution coefficient for each land cover class is calculated as:

$$Dj = \frac{\sum_i P_i(\frac{A_{IJ}}{A_i})}{\sum_i A_{ij}} \quad , W_j = \frac{D_j}{Max\,(D_j)} \tag{8}$$

where $W_j$is the weight of land cover class j, $D_j$is its population density, and $D$is the total population density. The population assigned to each fine-resolution land cover pixel is then estimated as:

$$P_{ik} = \frac{P_I * W_j}{\sum_{j=1}^{n} W_j} \tag{9}$$

where $P_i$is the total population in the original WorldPop grid and $P_{ij}$is the population allocated to land cover class $j$within that grid. Thus, land cover data do not independently generate population values, but redistribute the original population totals according to the relative residential capacity of each land cover class, while preserving the total population of the source grid.

2.6. Spatial Interaction Analysis

To peform spatial interaction from land cover model, the gravity model is used because it offers a transparent and interpretable way to relate origin mass, destination mass, and spatial separation (Fotheringham & O'Kelly, 1989; Wilson, 1971). Contemporary mobility literature shows that gravity-type models remain useful as baseline spatial interaction models, although their parameters and distance-decay assumptions should be treated carefully and interpreted relative to available data (Barbosa et al., 2018; Lenormand et al., 2016; Simini et al., 2012). The gravity model is therefore used here to estimate relative interaction potential between origin zone *i* and destination zone *j*:

$$I_{ij} = K\frac{O_i^{\alpha} D_j^{\beta}}{f(c_{ij})}, \tag{10}$$

where I_{ij} is the estimated spatial interaction between zones i and j, O_i is the origin mass, D_j is the destination population mass, C_{ij} is spatial separation or travel impedance, $f(C_{ij})$ is the distance-decay function, K is a scaling constant, and α and β are parameters controlling the influence of origin and destination population. This research using travel impedance based on the type of road network hierarchy. These table below is the type of road and its range of free flow speed (Kementrian Perhubungan, 2015):

Table 2. Road type and speed

Type	Range of Free Flow Speed	Typical Free Flow Speed
Arterial Road	90 – 70 km/h	80 km/h
Secondary Road	70 – 55 km/h	65 km/h
Local Road	55 – 40 km/h	45 km/h
Neighborhood Road	40 – 30 km/h	20 km/h

Source: *Kementrian Perhubungan (2015) modified*

For this study, both origin mass and destination mass are represented by population. The population value for each zone is estimated from built-up areas, including settlement and industrial built-up areas, so that the gravity model compares population-based interaction potential between zones rather than attraction based on land cover activity categories. Spatial separation can be measured using Euclidean distance, network distance, or travel time, depending on data availability. A common distance-decay function is:

$$f(c_{ij}) = c_{ij}^{\gamma}, \tag{11}$$

where γ is the distance-decay parameter. The same gravity-model structure is applied to both 2022 and 2042 so that interaction changes are caused by differences in population distribution derived from built-up land patterns and spatial impedance. To peform the model in this reseach is used GraviGIS Software.

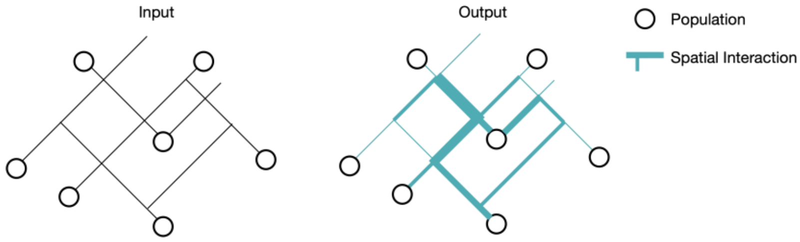

Figure 2. Conceptual of the gravity-based network in GraviGIS Software

3. Result and Discussion

3.1. Data pre-processing

a. Land Cover Data

The land cover layers were prepared from Landsat imagery for 2002 and 2022, reclassified into 6 categories, resampled to a uniform 30m cell, and clipped to the study-area boundary. The resulting maps show a clear gradient of built-up concentration along the Driyorejo–Surabaya corridor, while agricultural land remains dominant in Wringinanom and Kedamean. This configuration provided the calibrated input for the cellular-automata simulation.

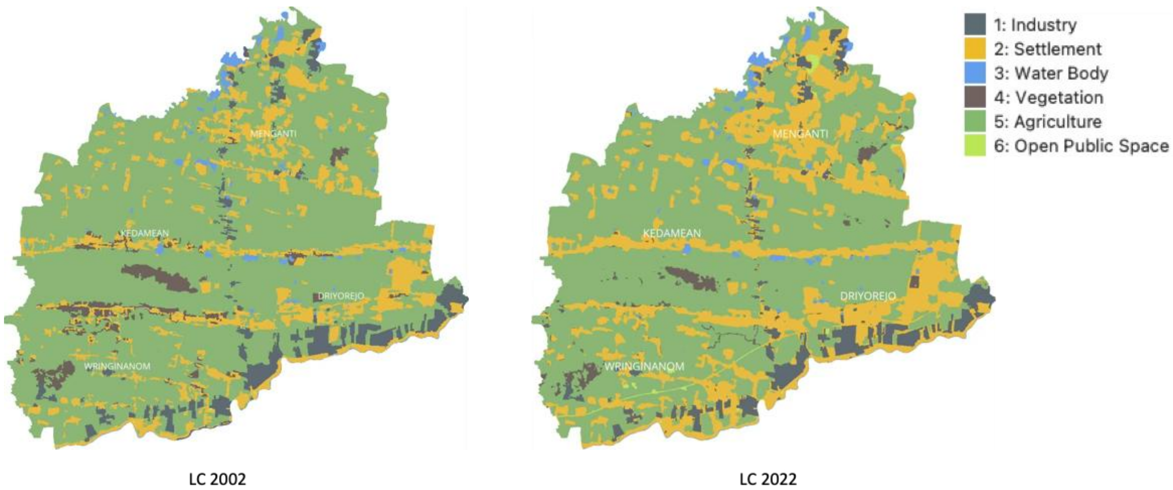

Figure 3. Land Cover 2002 and 2022

b. Driving factor and Constraint

Nine driving-factor layers were prepared as CA inputs: distance to existing built-up area, distance to the primary and secondary road network, distance to the exit toll-road, distance to industrial estates, distance to activity centers such as urban system, transport facility, public facility and tourism. Together these layers associated with peri-urban land-cover conversion in metropolitan corridors (Santé et al., 2010; Liu et al., 2017). In this case, the driving factor form Surabaya City is still used. Each layer was normalized to a comparable [0–1] suitability scale. Constraint layers such as water bodies, protected forest, and areas designated under the LP2B sustainable agricultural protection scheme, were encoded as binary restrictions preventing built-up conversion.

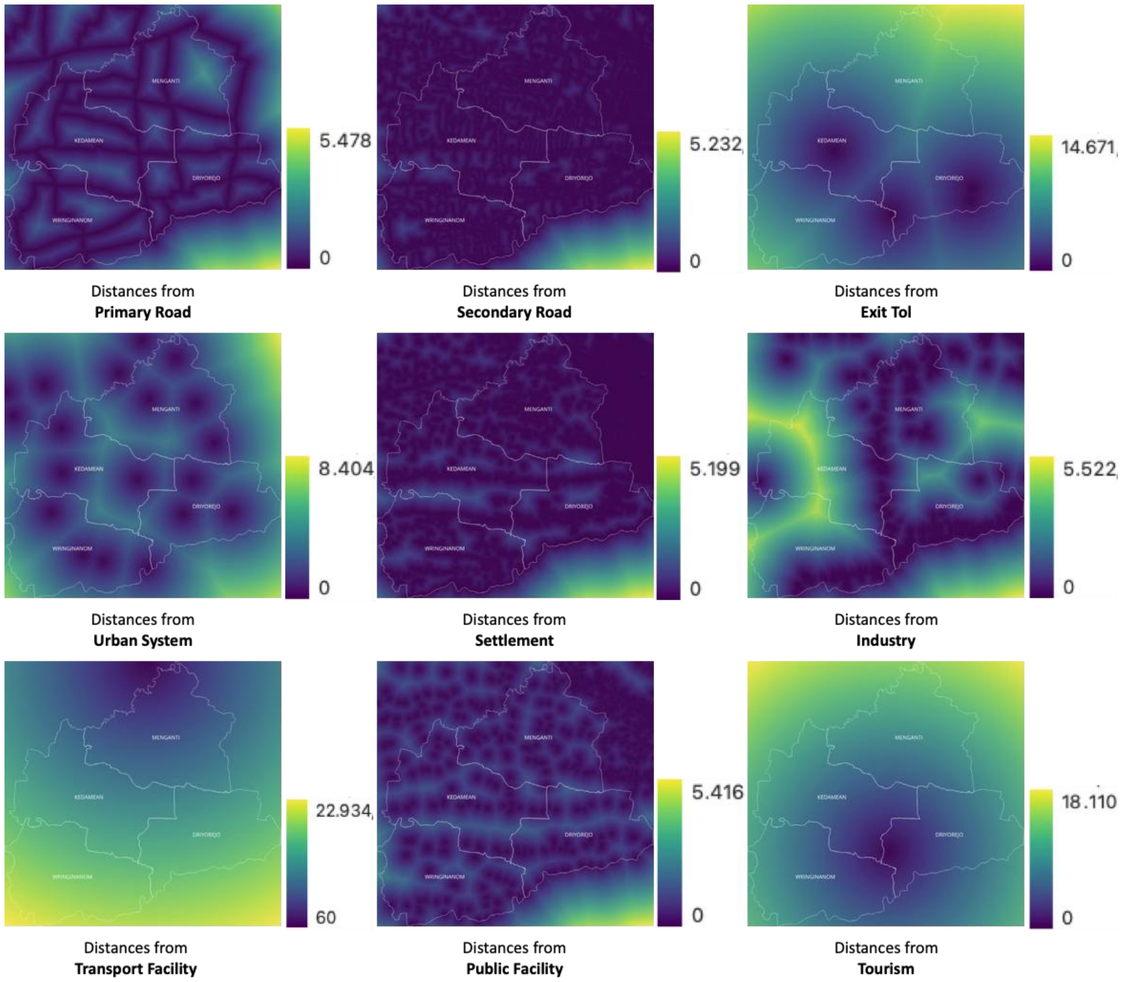

Figure 4. Distance Value from Driving Factor

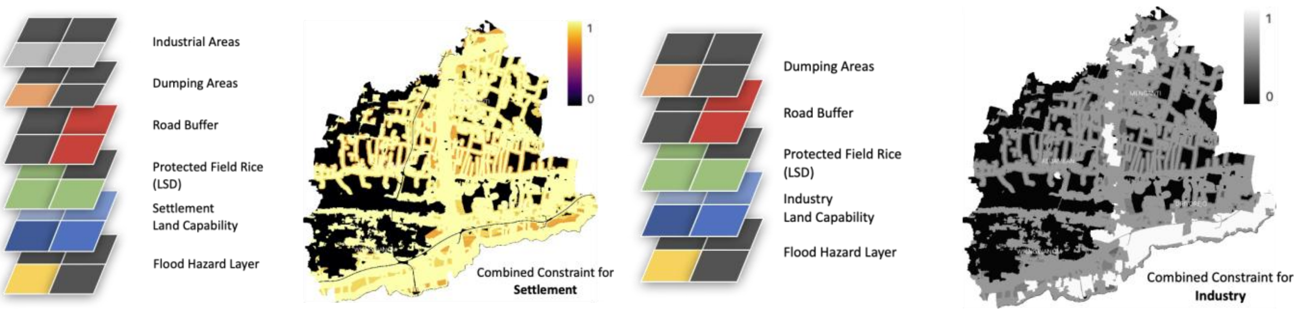

Figure 5. Constraint for each active land cover (a) constraint for settlement, (b) constraint for industry

Driving-factor weights were derived from an Analytic Hierarchy Process (AHP) with separate schemes for settlement and industry growth. The matrix consistency ratio was CR = 0.023, confirming the internal consistency of the pairwise comparisons. The industry scheme is dominated by industrial self-agglomeration (0.29), primary roads (0.21), and toll-road exits (0.18), reflecting the logistics-driven calculus of industrial location. Constraints — protected rice fields, forest, river boundaries, mangrove, mining, graveyards, open public space, and areas of low land capability or non-conforming spatial designation — are encoded as full restrictions (score = 1), with disaster-prone areas as a graded restriction (0.5). Road influence operates within buffers of 500 m for primary roads and 100 m for local roads.

Table 3. Scoring each driving factor and constraint

Settlement Driving Factor Score	
Exit Tol	0.06
Public Facility	0.12
Industry - Increase	0.03
Tourism	0.04
Settlement	0.25
Transport Facility	0.04
Secondary Road	0.26
Primary Road	0.12
Urban System	0.08

Industry Driving Factor Score	
Exit Tol	0.18
Public Facility	0.07
Industry	0.29
Tourism	0.01
Settlement	0.08
Transport Facility	0.05
Secondary Road	0.05
Primary Road	0.21
Urban System	0.06

Constraint Score	
Protected Field Rice	1
The effectiveness of the influence of the road network on growth > 500m for main roads and 100m for local and neighborhood roads	1
Disaster Areas	0.5
Land Capability	0.2
Land Suitability from Spatial Plan Document	1
Forest	1
Graveyard	1
River Boundary	1
Mining	1
Open Public Space (Park, Sport Field, etc)	1
Mangrove	1

c. Transition Potential Growth Maps with Constraint Zoning

Transition potential maps integrate the AHP-weighted driving factors with constraint zoning to identify cells eligible for settlement or industrial conversion. High-potential cells concentrate along the road and around buildup areas, while protected rice fields, forest, and other restricted zones appear as masked-out, non-convertible areas.

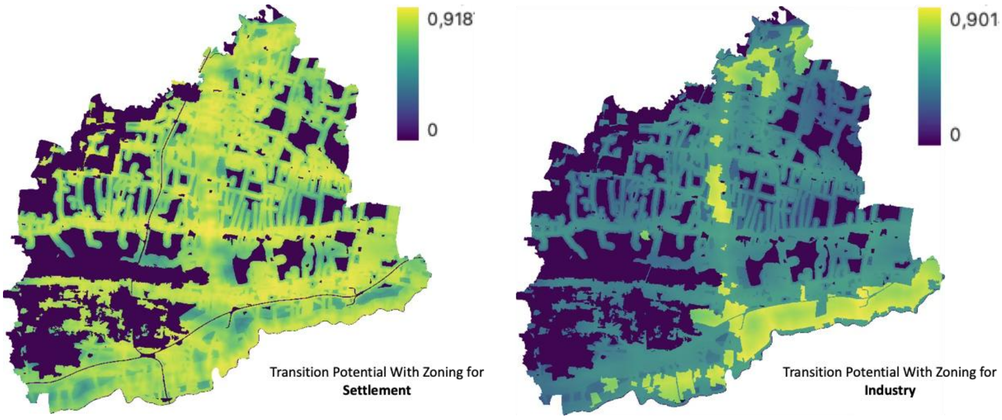

Figure 6. Transition potential maps of settlement and industry

d. Neighborhood Filter

A 3×3 Moore neighborhood operationalises local spillover effects, following established practice in urban CA modelling (Hagoort et al., 2008; Verburg, De Nijs, et al., 2004; White & Engelen, 1993). The sum operation aggregates built-up neighbour counts, capturing cumulative agglomeration pressure — equivalent to the enrichment-factor logic in neighbourhood-based CA (Verburg, De Nijs, et al., 2004)

1	1	1
1	1	1
1	1	1

Neighborhood Filter 3X3
sum operation

Figure 7. Neighbourhood Filter 3x3

e. Growth number Estimation

The 2042 growth demand was calibrated from the observed historical conversion trend. Annual rates of agricultural and undeveloped land transitioning to built-up use were derived from the 2002-2022 reference period and extrapolated over the 20-year horizon, yielding total settlement and industrial demands respectively (Verburg et al., 2002; Liu et al., 2017; Pratomoatmojo, 2018).

Table 4. Estimation settlement and industry growth

Areas	Settlemet Growth	Industry Growth
Gresik Selatan	393267	36101

3.2. Land Cover Change Simulation

The cellular-automata model was applied to the 2022 baseline to project land cover to 2042. The transition matrix (Figure. 8) shows substantial class restructuring over the projection horizon: Industrial cover expands from 2.54 to 4.79 ha (+88.6%), drawing primarily from agriculture and from a 10% displacement of existing settlement. Settlement grows from 9.00 to 12.44 ha (+38.2%), absorbing agricultural and vegetation land. Vegetation declines by 30.1% and agriculture by 37.4%, while Water body and Open Public Space (OPS) was unchanged.

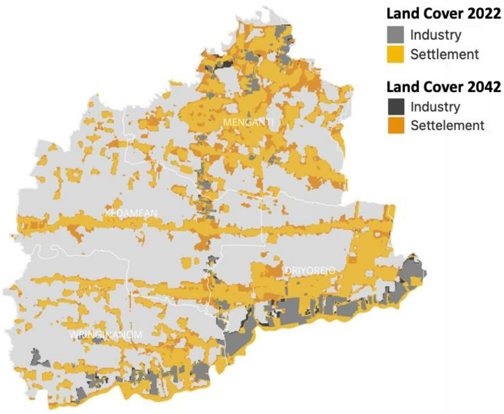

Land-cover class	2022 (ha)	2042 (ha)	Δ ha	Δ % (visual)
Industry	2.54	4.79	+2.25	+88.6%
Settlement	9.00	12.44	+3.44	+38.2%
Water body	6.58	6.58	0.00	0.0%
Vegetation	5.58	3.90	-1.68	-30.1%
Agriculture	10.72	6.71	-4.01	-37.4%
OPS	1.27	1.27	0.00	0.0%
Total	35.69	35.69	0.00	—

Figure 8. Land Cover change 2022 – 2042
Source: LanduseSim Result

The simulation achieved an overall accuracy of 83%, which falls within the range reported as acceptable for cellular-automata land-use change studies (Foody, 2002; Pontius & Millones, 2011). Overall accuracy measures the proportion of cells whose simulated class matches the observed class, providing a cell-by-cell indicator of model fidelity. In the CA context, this value indicates that the calibrated transition rules and driving-factor weights capture the dominant land-cover dynamics with sufficient reliability to support the 2042 scenario projection.

3.3. Population Distribution Model

Only the two built-up classes receive population; Water body, Vegetation, Agriculture, and Open Public Space are forced to zero (Force = 1) because they do not represent residential surface. The computed coefficients are 0.540 for Settlement and 0.459 for Industry, meaning that approximately 54% and 46% of each WorldPop grid's population are allocated to settlement and industrial pixels respectively, in proportion to their relative residential density. The result shows population concentrated along the Driyorejo–Menganti corridor, mirroring the settlement gradient observed in the underlying land-cover map and confirming that the redistribution preserves the spatial logic of the 2022 baseline.

Table 5. Population Estimation

LC Code	Total Grid	Population	Pop Density	Coefficient	Force
1. Settlement	137357	59864	0,435	0,459	0
2. Industry	668907	343058	0,512	0,540	0
3. Water body	35954	0.0	0.0	0.0	1
4. Vegetation	43528	0.0	0.0	0.0	1
5. Agriculture	1634887	0.0	0.0	0.0	1
6. OPS	9916	0.0	0.0	0.0	1

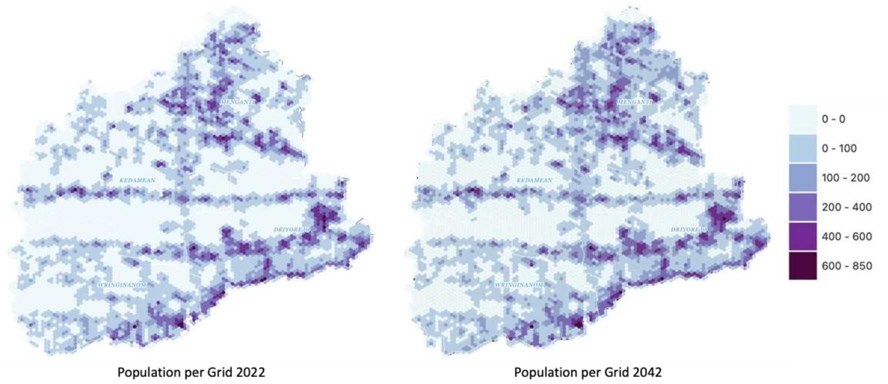

Figure 9. Population Spatial Distribution 2022 - 2042

Aggregating the disaggregated population to the village and subdistrict scale (Figure 10) reveals the spatial structure of projected growth across the four subdistricts of Southern Gresik. Driyorejo holds the largest absolute population in both years (152,819 in 2022 → 171,210 in 2042) but records the slowest compound annual growth rate (CAGR = 0.57%/yr). In contrast, Kedamean and Menganti the smaller subdistricts further from the Surabaya core show the fastest projected CAGRs at 1.58%/yr and 1.39%/yr respectively. The regional pooled CAGR is 1.01%/yr. This inverse size–growth relationship, in which the largest and innermost subdistrict grows most slowly while the smaller outer subdistricts expand most rapidly, is consistent with the staged peri-urbanisation pattern documented in other metropolitan fringes, where the inner ring saturates first and growth diffuses outward (Firman, 2017; Rustiadi et al., 2021).

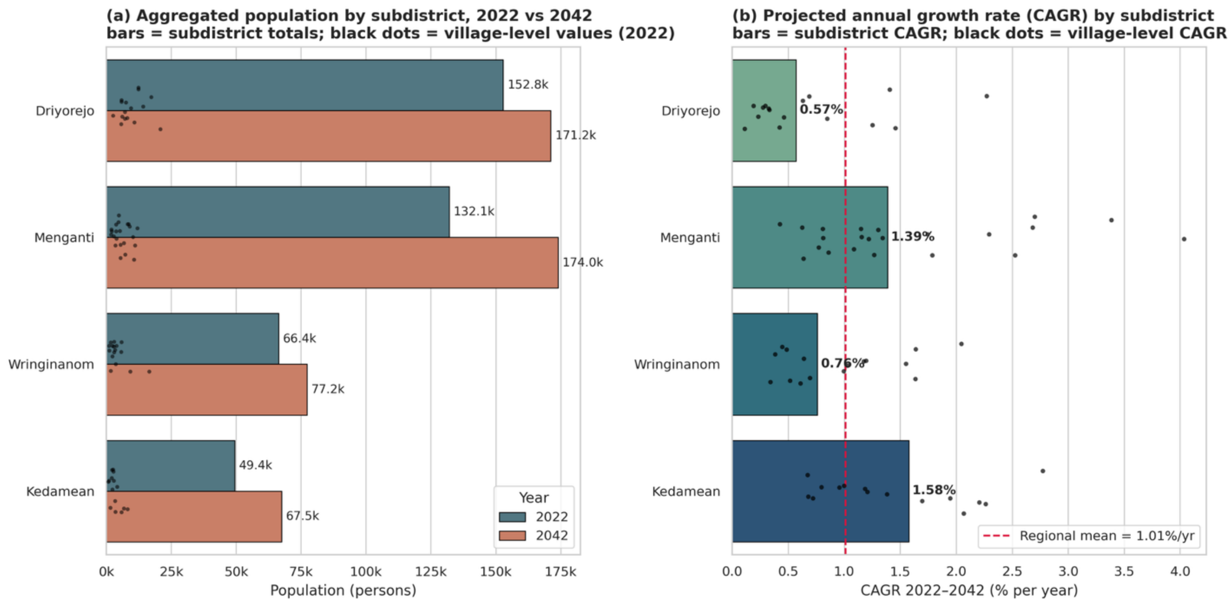

Figure 10. Population aggregation and projected Growth (n = 69 villages, 4 subdistricts)

3.4. Spatial Interaction Model

The network-level visualisation of gravity-derived interaction reveals a clear spatial concentration of inter-zonal flows along the principal north–south corridor of Southern Gresik and a substantial intensification between 2022 and 2042. In the 2022 baseline, interaction is dominated by a single high-flow corridor along Jalan Raya Kedamean. By 2042, this pattern strengthens and broadens: Jalan Raya Driyorejo and Jalan Raya Petiken emerge as additional very-high-flow segments, joining Jalan Raya Kedamean as the principal interaction corridors linking the southern subdistricts to the Surabaya core. The secondary and local road network retains moderate-to-low interaction intensity throughout. This indicates that the projected growth in interaction potential is not distributed evenly across the network but concentrates on a small number of arterial corridors.

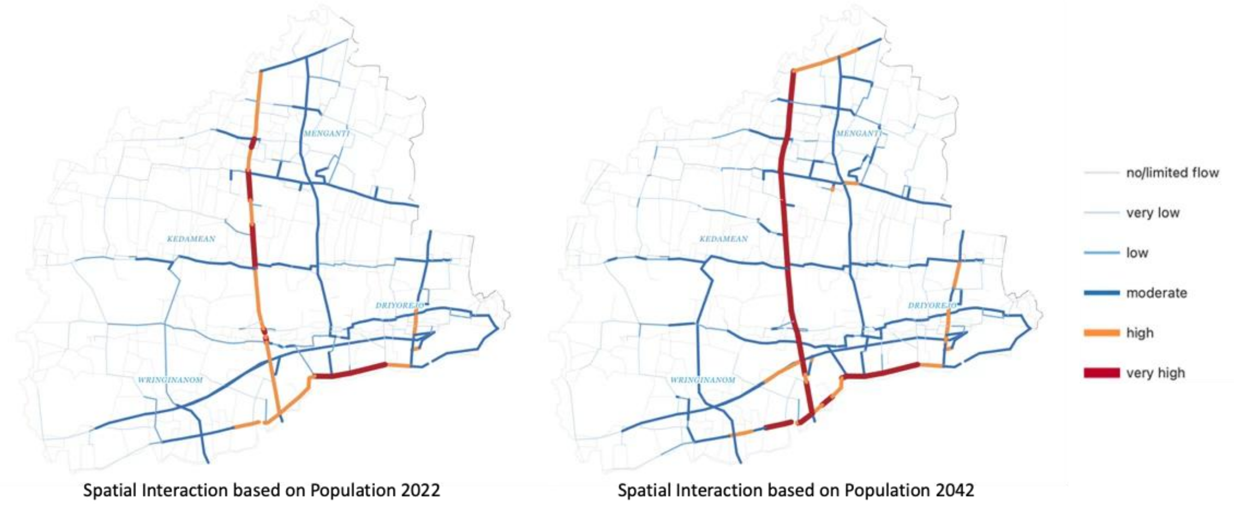

Figure 11. Spatial Interaction 2022 - 2042
Source: GraviGIS Result

The comparative analysis shows four patterns. The interaction hierarchy is preserved but compressed: Driyorejo remains dominant (341 → 458), yet the gap with Kedamean narrows from 3.2× to 2.6×. Interaction grows roughly twice as fast as population in every subdistrict (regional CAGR 1.95%/yr vs 1.01%/yr). Per-kilometre interaction intensity rises across all four units (Driyorejo: 2.03 → 2.72; Kedamean: 0.64 → 1.05). The interaction-to-population elasticity exceeds unity everywhere — E = 2.84, 2.28, 2.15, and 1.75 for Driyorejo, Wringinanom, Menganti, and Kedamean respectively (regional E = 1.93) — confirming that the projected interaction increase cannot be attributed to population growth alone.

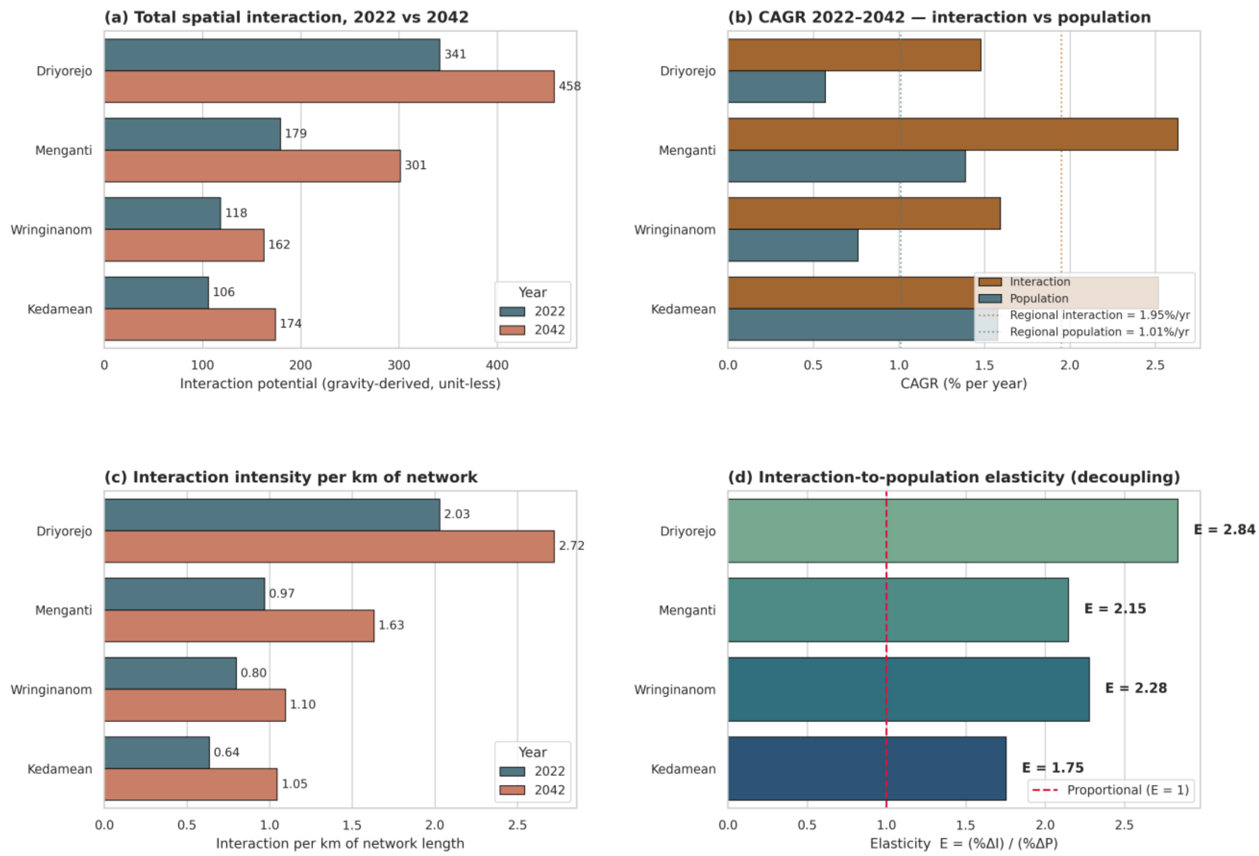

Figure 2. Spatial Interaction based on network comparative analysis

3.5. Discussion

The simulation shows that urban growth in Southern Gresik is not an isolated local process but part of the expansion of Greater Surabaya. Recent studies identify the Surabaya–Gresik corridor as a major axis of metropolitan development shaped by industrial agglomeration, arterial roads, toll access, and proximity to the urban core (Aulia, 2025; Katherina & Indraprahasta, 2019; Purwono et al., 2024; Santoso et al., 2026). This explains why projected settlement and industrial growth concentrates around existing built-up areas and transport infrastructure. Such a pattern confirms the peri-urban character of Southern Gresik, where urban, industrial, agricultural, and rural functions coexist within a rapidly changing landscape (Pahlevi et al., 2023; Rohmadiani et al., 2020; Sari & Santoso, 2017). The projected loss of agricultural and vegetated land therefore represents the continued absorption of rural land into the metropolitan system, particularly in locations with strong accessibility and development pressure (Liu et al., 2017; Rahmadani et al., 2025). Similar CA-based studies show that unconstrained corridor development commonly produces fragmented built-up expansion and greater agricultural conversion, while spatial restrictions can redirect growth toward more suitable locations (Arfiansyah et al., 2024; Santé et al., 2010). The simulation consequently provides an early indication of where development control and land protection need to be strengthened.

Population redistribution reinforces this outward transformation. This condition is consistent with Indonesian metropolitan expansion, in which growth initially accumulates near the core before moving toward more distant transitional areas (Firman, 2017; Santoso et al., 2026). Integrating land-cover projections with dasymetric population redistribution is important because infrastructure demand depends not only on total population growth but also on its location and spatial concentration (Diogo et al., 2023). The projected outward shift may expand the settlement system, but it can also widen the separation between housing, employment, and higher-order services. Commuting-based analysis of the Surabaya metropolitan region shows that these functional relationships already extend beyond contiguous urban land and administrative boundaries (Aritenang et al., 2025). Without a parallel decentralization of employment, services, and public transport, population growth in the outer fringe may therefore reinforce dependence on city center (Aritenang et al., 2025; Pyrohova et al., 2025) such as Surabaya and established centers in Driyorejo and Menganti.

The gravity model adds a relational perspective by showing how the projected population pattern may alter interaction between zones and concentrate pressure on the road network. Gravity-based interaction increases with origin and destination mass but declines with network impedance, making it suitable for comparing the relative connectivity of zones under different population scenarios (Roy & Thill, 2004; Wang & Chen, 2022; Wilson, 1971). The projected strengthening of Jalan Raya Kedamean, Jalan Raya Driyorejo, and Jalan Raya Petiken indicates that population decentralization does not necessarily disperse movement pressure; new interactions remain channeled through a limited number of strategic corridors. This is consistent with earlier evidence that relationships between Surabaya and its peri-urban areas generate concentrated transport and environmental pressures along the metropolitan network (Santoso et al., 2019). The faster growth of interaction relative to population also suggests that network pressure is influenced not only by demographic increase but by the location of new residents. Assigning gravity-derived interaction to individual road segments therefore converts projected population change into a practical corridor-screening indicator for public transport planning, junction improvement, capacity management, and land-use control. The results should not be interpreted as observed traffic volumes because the model does not include calibrated trip generation, mode choice, congestion, or observed origin destination flows. Nevertheless, as a comparative planning instrument, it identifies where urban expansion and population redistribution are most likely to strengthen future mobility pressure.

4. Conclusion

This study demonstrates that future urban growth in Southern Gresik should be understood as a coupled process of land conversion, population redistribution, and changing spatial interaction within the Greater Surabaya metropolitan system. By integrating a validated cellular-automata simulation, dasymetric population redistribution, and a network-based gravity model, the study moves beyond conventional land-cover projection and provides a practical means of tracing how peri-urban expansion may translate into corridor-specific mobility pressure. The results imply that outward population growth does not necessarily produce a more balanced metropolitan structure. Without coordinated decentralization of employment, services, and public transport, development in the outer fringe may intensify dependence on a limited number of arterial corridors while accelerating the conversion of agricultural and vegetated land. Spatial and transport policies should therefore be formulated jointly, with priority given to development control, protection of strategic non-built-up land, strengthening of emerging service centers, and early intervention along corridors showing rapidly increasing interaction potential. The gravity-model outputs are not forecasts of actual traffic volumes, but comparative indicators of where future spatial dependence may intensify under the projected growth scenario. Within this limitation, the proposed framework offers a transferable planning approach for data-constrained peri-urban regions, enabling land-development scenarios to be evaluated according to their likely implications for population distribution and network pressure. Future research should strengthen this framework through calibrated origin–destination data, alternative land-use scenarios, and explicit testing of public-transport and growth-management interventions.

References

Aburas, M. M., Ho, Y. M., Ramli, M. F., & Ash'aari, Z. H. (2016). The simulation and prediction of spatio-temporal urban growth trends using cellular automata models: A review. International Journal of Applied Earth Observation and Geoinformation, 52, 380–389. https://doi.org/10.1016/j.jag.2016.07.007

Acheampong, R. A., & Silva, E. (2015). Land use–transport interaction modeling: A review of the literature and future research directions. Journal of Transport and Land Use, 8(3). https://doi.org/10.5198/jtlu.2015.806

Arfiansyah, D., Hawken, S., Zlatanova, S., & Han, H. (2024). Cellular automata modelling to simulate patterns of urban growth for Nusantara: Indonesia's new capital. Spatial Information Research, 32(6), 829–849. https://doi.org/10.1007/s41324-024-00599-5

Aritenang, A. F., Ginting, S. R. S., & Sakti, A. D. (2025). Metropolitan spatial structure based on commuting pattern: A comparison between Jakarta and Surabaya metropolitans. International Journal of Urban Sciences, 29(2), 503–521. https://doi.org/10.1080/12265934.2024.2358101

Aulia, B. U. (2025). Ekspansi Perkotaan di Surabaya Metropolitan Area: Alami atau Terrencana? Jurnal Penataan Ruang, 20(2), 164–173. https://doi.org/10.12962/j2716179X.v20i2.4194

Barbosa, H., Barthelemy, M., Ghoshal, G., James, C. R., Lenormand, M., Louail, T., Menezes, R., Ramasco, J. J., Simini, F., & Tomasini, M. (2018). Human mobility: Models and applications. Physics Reports, Human Mobility: Models and Applications, 734, 1–74. https://doi.org/10.1016/j.physrep.2018.01.001

Batty, M., & Xie, Y. (1994). From Cells to Cities. Environment and Planning B: Planning and Design, 21(7), S31–S48. https://doi.org/10.1068/b21S031

Clarke, K. C., Hoppen, S., & Gaydos, L. (1997). A Self-Modifying Cellular Automaton Model of Historical Urbanization in the San Francisco Bay Area. Environment and Planning B: Planning and Design, 24(2), 247–261. https://doi.org/10.1068/b240247

Couclelis, H. (1985). Cellular Worlds: A Framework for Modeling Micro—Macro Dynamics. Environment and Planning A: Economy and Space, 17(5), 585–596. https://doi.org/10.1068/a170585

Diogo, V., Jacobs-Crisioni, C., Baranzelli, C., & Lavalle, C. (2023). Integrated Spatial Simulation of Population and Urban Land Use: A Pan-European Model Validation. Applied Spatial Analysis and Policy, 16(4), 1463–1492. https://doi.org/10.1007/s12061-023-09518-x

Firman, T. (2009). The continuity and change in mega-urbanization in Indonesia: A survey of Jakarta–Bandung Region (JBR) development. Habitat International, 33(4), 327–339. https://doi.org/10.1016/j.habitatint.2008.08.005

Firman, T. (2017). The urbanisation of Java, 2000–2010: Towards 'the island of mega-urban regions.' Asian Population Studies, 13(1), 50–66. https://doi.org/10.1080/17441730.2016.1247587

Foody, G. M. (2002). Status of land cover classification accuracy assessment. Remote Sensing of Environment, 80(1), 185–201. https://doi.org/10.1016/S0034-4257(01)00295-4

Fotheringham, A., & O'Kelly, M. E. (1989). Spatial Interaction Models Formulations and Applications. Scientific Research Publishing. https://www.scirp.org/reference/referencespapers?referenceid=2286794

Geurs, K. T., & van Wee, B. (2004). Accessibility evaluation of land-use and transport strategies: Review and research directions. Journal of Transport Geography, 12(2), 127–140. https://doi.org/10.1016/j.jtrangeo.2003.10.005

Gresik Regency Government. (2011). Peraturan Daerah Kabupaten Gresik Nomor 8 Tahun 2011 tentang Rencana Tata Ruang Wilayah Kabupaten Gresik Tahun 2011–2031.

Güneralp, B., Reba, M., Hales, B. U., Wentz, E. A., & Seto, K. C. (2020). Trends in urban land expansion, density, and land transitions from 1970 to 2010: A global synthesis. Environmental Research Letters, 15(4), 044015. https://doi.org/10.1088/1748-9326/ab6669

Hagoort, M., Geertman, S., & Ottens, H. (2008). Spatial externalities, neighbourhood rules and CA land-use modelling. The Annals of Regional Science, 42(1), 39–56. https://doi.org/10.1007/s00168-007-0140-8

Haynes, K. E., & Fotheringham, A. S. (1984). Gravity and Spatial Interaction Models. Sage Publication.

Hudalah, D., & Firman, T. (2012). Beyond property: Industrial estates and post-suburban transformation in Jakarta Metropolitan Region. Cities, 29(1), 40–48. https://doi.org/10.1016/j.cities.2011.07.003

Iacono, M., Levinson, D., & El-Geneidy, A. (2008). Models of Transportation and Land Use Change: A Guide to the Territory. Journal of Planning Literature, 22(4), 323–340. https://doi.org/10.1177/0885412207314010

JICA. (2007). The Study for Development of The Greater Surabaya Metropolitan Ports in the Republic of Indonesia (Existing Conditions and Issues, Vol. 1). Japan International Cooperation Agency.

Katherina, L. K., & Indraprahasta, G. S. (2019). Urbanization Pattern in Indonesia's Secondary Cities: Greater Surabaya and Its Path toward a Megacity. IOP Conference Series: Earth and Environmental Science, 338(1), 012018. https://doi.org/10.1088/1755-1315/338/1/012018

Kementrian Perhubungan. (2015). Peraturan Menteri Perhubungan Republik Indonesia, Nomor PM 111 tahun 2015 tentang Tata Cara Penetapan Batas Kecepatan.

Lenormand, M., Bassolas, A., & Ramasco, J. J. (2016). Systematic comparison of trip distribution laws and models. Journal of Transport Geography, 51, 158–169. https://doi.org/10.1016/j.jtrangeo.2015.12.008

Li, X., & Yeh, A. G.-O. (2000). Modelling sustainable urban development by the integration of constrained cellular automata and GIS. International Journal of Geographical Information Science, 14(2), 131–152. https://doi.org/10.1080/136588100240886

Li, X., & Yeh, A. G.-O. (2002). Neural-network-based cellular automata for simulating multiple land use changes using GIS. International Journal of Geographical Information Science, 16(4), 323–343. https://doi.org/10.1080/13658810210137004

Li, Z., Fan, Z., & Shen, S. (2018). Urban Green Space Suitability Evaluation Based on the AHP-CV Combined Weight Method: A Case Study of Fuping County, China. Sustainability, 10(8), 2656. https://doi.org/10.3390/su10082656

Liang, X., Guan, Q., Clarke, K. C., Liu, S., Wang, B., & Yao, Y. (2021). Understanding the drivers of sustainable land expansion using a patch-generating land use simulation (PLUS) model: A case study in Wuhan, China. Computers, Environment and Urban Systems, 85, 101569. https://doi.org/10.1016/j.compenvurbsys.2020.101569

Lin, J., Li, X., Wen, Y., & He, P. (2023). Modeling urban land-use changes using a landscape-driven patch-based cellular automaton (LP-CA). Cities, 132, 103906. https://doi.org/10.1016/j.cities.2022.103906

Liu, X., Liang, X., Li, X., Xu, X., Ou, J., Chen, Y., Li, S., Wang, S., & Pei, F. (2017). A future land use simulation model (FLUS) for simulating multiple land use scenarios by coupling human and natural effects. Landscape and Urban Planning, 168, 94–116. https://doi.org/10.1016/j.landurbplan.2017.09.019

Mcgee, T. (1991). The emergence of desakota regions in Asia: Expanding a hypothesis.

Pahlevi, M. R., Dinanti, D., Subagiyo, A., Qomariyah, Y., & Varo, J. (2023). The Relationship Between Community Characteristics and Urban Sprawl in Driyorejo Sub-District, Gresik Regency, Indonesia. Regional and Rural Studies, 1(1), 22–31. https://doi.org/10.21776/rrs.v1i1.6

Pontius, R. G., & Millones, M. (2011). Death to Kappa: Birth of quantity disagreement and allocation disagreement for accuracy assessment. International Journal of Remote Sensing, 32(15), 4407–4429. https://doi.org/10.1080/01431161.2011.552923

Pratomoatmojo, N. A. (2018a). LanduseSim Algorithm: Land use change modelling by means of Cellular Automata and Geographic Information System. IOP Conference Series: Earth and Environmental Science, 202, 012020. https://doi.org/10.1088/1755-1315/202/1/012020

Pratomoatmojo, N. A. (2018b). Permodelan Perubahan Penggunaan Lahan Berbasis Cellular Automata dan Sistem Informasi Geografis dengan Menggunakan LanduseSim. Jurnal Penataan Ruang, 13(1), 26. https://doi.org/10.12962/j2716179X.v13i1.7064

Purwono, N., Susetyo, D., Rijal, S., Syaripah, G., & Munawaroh, S. (2024). Assessing urban growth in Greater Surabaya using Google Earth Engine: An evaluation of built-up area expansion in Indonesian secondary cities. Journal of the Geographical Institute Jovan Cvijic, SASA, 74(1), 127–138. https://doi.org/10.2298/IJGI230608004P

Pyrohova, S., Nguyen, B. H., Rambaldi, A. N., Wohland, P., Bernard, A., Lieske, S., & Corcoran, J. (2025). An Integrated Land-Use, Population, and Transport Model for Strategic Regional Planning: From Research to Operational Practice. Applied Spatial Analysis and Policy, 18(3), 92. https://doi.org/10.1007/s12061-025-09691-1

Rahmadani, C. S. N., Zain, A. F. M., & Indraprahasta, G. S. (2025). Urban Sprawl and Its Impacts on Land Cover Change in the Outskirts of the Surabaya Metropolitan Area. Jurnal Wilayah Dan Lingkungan, 13(3), 61–71. https://doi.org/10.14710/jwl.13.3.61-71

Rohmadiani, L. D., Kunce, Y. A., & Rachmawanti, I. D. (2020). Fenomena Urban Sprawl Wilayah Pembangunan Gresik Selatan. Jurnal Penataan Ruang, 15(1), 1. https://doi.org/10.12962/j2716179X.v15i1.6722

Roy, J. R., & Thill, J. C. (2004). Spatial interaction modelling. Papers in Regional Science, 83(1), 339–361. https://doi.org/10.1007/s10110-003-0189-4

Rustiadi, E., Pravitasari, A. E., Setiawan, Y., Mulya, S. P., Pribadi, D. O., & Tsutsumida, N. (2021). Impact of continuous Jakarta megacity urban expansion on the formation of the Jakarta-Bandung conurbation over the rice farm regions. Cities, 111, 103000. https://doi.org/10.1016/j.cities.2020.103000

Saaty, T. L., & Vargas, L. G. (2012). Models, methods, concepts & applications of the analytic hierarchy process (2nd ed). Springer.

Santé, I., García, A. M., Miranda, D., & Crecente, R. (2010). Cellular automata models for the simulation of real-world urban processes: A review and analysis. Landscape and Urban Planning, 96(2), 108–122. https://doi.org/10.1016/j.landurbplan.2010.03.001

Santoso, E. B., Aulia, B. U., Aninditya, D. N., & Handayeni, K. D. M. (2019). Spatial interaction between urban and peri-urban regions of Surabaya metropolitan area and its impact to the carbon footprint of transportation sector. IOP Conference Series: Earth and Environmental Science, 340(1), 012017. https://doi.org/10.1088/1755-1315/340/1/012017

Santoso, E. B., Putra, D. W., Iswi, A., & Wardhana, R. D. S. B. (2026). Development of greater Surabaya metropolitan 2000–2023: Metropolitan understanding using functional urban area at village scale. Frontiers in Sustainable Cities, 8, 1760759. https://doi.org/10.3389/frsc.2026.1760759

Sari, K. D. R., & Santoso, E. B. (2017). Analisis Keterkaitan Wilayah Peri Urban di Kabupaten Gresik dengan Wilayah Desa-Kota di Sekitarnya. Jurnal Teknik ITS, 6(2), C150–C155. https://doi.org/10.12962/j23373539.v6i2.24971

Seto, K. C., Güneralp, B., & Hutyra, L. R. (2012). Global forecasts of urban expansion to 2030 and direct impacts on biodiversity and carbon pools. Proceedings of the National Academy of Sciences of the United States of America, 109(40), 16083–16088. https://doi.org/10.1073/pnas.1211658109

Simini, F., González, A., & Maritan, A. (2012). A universal model for mobility and migration patterns. 484, 96–100. https://doi.org/https://doi.org/10.1038/nature10856

Tobler, W. R. (1970). A Computer Movie Simulating Urban Growth in the Detroit Region. Economic Geography, 46, 234–240. https://doi.org/10.2307/143141

Van Vliet, J., Bregt, A. K., & Hagen-Zanker, A. (2011). Revisiting Kappa to account for change in the accuracy assessment of land-use change models. Ecological Modelling, 222(8), 1367–1375. https://doi.org/10.1016/j.ecolmodel.2011.01.017

Verburg, P. H., De Nijs, T. C. M., Ritsema Van Eck, J., Visser, H., & De Jong, K. (2004). A method to analyse neighbourhood characteristics of land use patterns. Computers, Environment and Urban Systems, 28(6), 667–690. https://doi.org/10.1016/j.compenvurbsys.2003.07.001

Verburg, P. H., Schot, P. P., Dijst, M. J., & Veldkamp, A. (2004). Land use change modelling: Current practice and research priorities. GeoJournal, 61(4), 309–324. https://doi.org/10.1007/s10708-004-4946-y

Wang, Z., & Chen, Y. (2022). Exploring Spatial Patterns of Interurban Passenger Flows Using Dual Gravity Models. Entropy, 24(12), 1792. https://doi.org/10.3390/e24121792

Wegener, M. (2004). Overview of Land Use Transport Models. In D. A. Hensher, K. J. Button, K. E. Haynes, & P. R. Stopher (Eds.), Handbook of Transport Geography and Spatial Systems (Vol. 5, p. 0). Emerald Group Publishing Limited. https://doi.org/10.1108/9781615832538-009

White, R., & Engelen, G. (1993). Cellular Automata and Fractal Urban Form: A Cellular Modelling Approach to the Evolution of Urban Land-Use Patterns. Environment and Planning A: Economy and Space, 25(8), 1175–1199. https://doi.org/10.1068/a251175

Wilson, A. G. (1971). A Family of Spatial Interaction Models, and Associated Developments. Environment and Planning A: Economy and Space, 3(1), 1–32. https://doi.org/10.1068/a030001

Winarso, H., Hudalah, D., & Firman, T. (2015). Peri-urban transformation in the Jakarta metropolitan area. Habitat International, 49, 221–229. https://doi.org/10.1016/j.habitatint.2015.05.024

Wu, F. (2002). Calibration of stochastic cellular automata: The application to rural-urban land conversions. International Journal of Geographical Information Science, 16(8), 795–818. https://doi.org/10.1080/13658810210157769